CONTROL OF LASER RADIATION PARAMETERS

PACS numbers: 42.55.Px; 42.62.Eh; 42.79.Jq
DOI: 10.1070/QE2007v037n11ABEH013552

Phase-sensitive detection of optical resonances by using an acousto-optic modulator in the Raman – Nath diffraction mode

V.N. Baryshev, Yu.S. Domnin, L.N. Kopylov

***Abstract*. A new method for frequency control of an external cavity diode laser without direct modulation of the injection current is proposed. The Pound – Drever optical heterodyne technique or the method of frequency control by frequency-modulated sidebands, in which an acousto-optic modulator operating in the Raman – Nath diffraction mode is used as an external phase modulator, can be employed to obtain error signals upon automatic frequency locking of the diode laser to the saturated absorption resonances within the D_2 line of cesium atoms or to the optical cavity resonances.**

Keywords: *laser, Pound – Drever technique, acousto-optic modulator, Raman – Nath diffraction.*

1. Introduction

The reduction of the frequency noise in semiconductor lasers is an important problem in various fields of science and technology such as nonlinear laser spectroscopy, metrology of microwave and optical quantum frequency standards on cold atoms, and stabilisation and calibration of femtosecond optical frequency combs. The width of the emission spectrum of an unstabilised external cavity diode laser (ECDL) is approximately a few megahertz and is caused by mechanical and acoustic vibrations of the external cavity. Such frequency fluctuations can be eliminated by using the electron feedback in the injection current of a laser diode (LD). Errors signals in extremely high-speed servo-loops are obtained at present by the method of frequency-modulated (FM) sidebands or the Pound – Drever technique [1, 2], in which an electrooptical modulator (EOM) is used as an external phase modulator.

It was found [3] that an acousto-optic modulator (AOM) operating in the Raman – Nath mode can be used as an external phase modulator in the Pound – Drever FM sideband technique to expand the input single-mode radiation of an LD into a FM and spatially separated optical spectrum. In the case of sinusoidal modulation and normal incidence of incident radiation, the AOM can be used to generate frequency sidebands located spatially symmetrically with respect to the optical beam at the carrier frequency. The sinusoidal modulation at the acoustic wave frequency Ω leads to the generation of sidebands at frequencies multiple of Ω around the central optical frequency ω. The electric field E of the optical beam propagated through the AOM is described by the known expression [4]

$$E = E_0 \exp\{\mathrm{i}[\omega t + m\sin(\Omega t)]\} = E_0\left[\sum_{k=0}^{\infty} J_k(m)\exp(\mathrm{i}k\Omega t) + \sum_{k=1}^{\infty}(-1)^k J_k(m)\exp(-\mathrm{i}k\Omega t)\right]\exp(\mathrm{i}\omega t).$$

The spectrum of the phase-modulated electric field is determined by the Bessel functions. The amplitude of the kth sideband at the frequency $\omega + k\Omega$ is proportional to $J_k(m)$, where $J_k(m)$ is the kth-order Bessel function and m is the modulation index. The diffraction angle ϑ_k for the kth sideband is determined from the relation $\sin\vartheta_k = k\lambda/\Lambda$, where λ and Λ are the light and acoustic wavelengths, respectively.

In this paper, we describe a new method for the frequency stabilisation of an ECDL without direct modulation of the injection current. The Pound – Drever technique or the method of frequency control by FM sidebands, in which an AOM operating in the Raman – Nath diffraction mode is used as an external phase modulator, is employed to obtain error signals in extremely high-speed servo-loops upon automatic frequency locking of the ECDL to the saturated absorption resonances within the D_2 absorption line of cesium atoms or to resonances of a high-Q optical cavity.

2. Experimental setup and results

Figure 1 shows the scheme of the experimental setup. Laser diodes SDL-5422 (USA) and IDL150S-850 (Polyus Research Institute, Russia) with an external cavity formed by a diffraction grating in Littrow mounting provided tunable single-frequency radiation at 851 nm. Modulation was produced by an ISOMET 1205-C2 AOM with a central operating frequency of 80 MHz and a modulation band of 40 MHz to which a 40-mW signal was applied from a HF generator at the frequency (varied from 30 to 40 MHz) considerably exceeding the natural width (5 MHz) of optical transitions within the D_2 absorption line of cesium atoms.

V.N. Baryshev, Yu.S. Domnin, L.N. Kopylov All-Russian Research Institute of Physicotechnical and Radiotechnical Measurements, 141570 Mendeleevo, Moscow region, Russia;
e-mail: barychev@aspnet.ru

Received 1 March 2007
Kvantovaya Elektronika **37** (11) 1006 – 1010 (2007)
Translated by M.N. Sapozhnikov

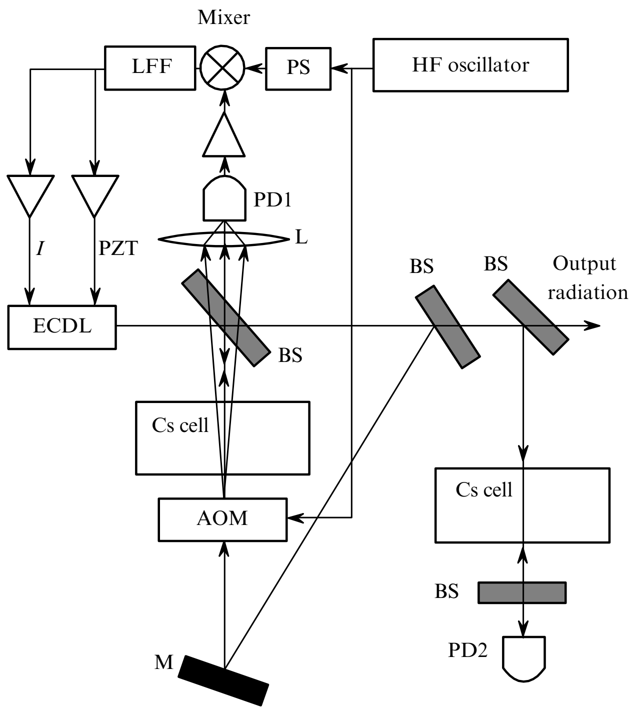

Figure 1. Scheme o the experimental setup: (PZT) piezoceramic transducer; (PS) phase shifter; (BS) beamsplitter; (L) lens; (M) mirror; (PD1, PD2) photodetectors; (LFF) low-frequency filter; (*1*) injection current.

The spatially and spectrally separated output beams of the AOM were used as probe beams for saturated absorption spectroscopy in a magnetically shielded cell with saturated cesium vapour at room temperature and were focused on a fast photodetector PD1. For the modulation parameters chosen and the appropriate alignment of the input optical beam, the output radiation of the AOM consisted only of three beams corresponding to the carrier and two nearest sidebands of the ±1st diffraction order with the diffraction angle $\vartheta_{\pm 1} \simeq \pm 0.5^{\circ}$. The ratio of the power of each of the sidebands in the ±1st diffraction order to the power of the carrier component in front of the input window of the cesium cell was $P_{\pm}/P_0 = 65$ μW/1.75 mW $\simeq 0.04$.

High-frequency beats were detected in a heterodyne Mini-Circuits SRA-1 mixer, whose output constant signal was used as the error signal in the fast electronic feedback circuit. Figures 2 and 3 show error signals of the disperse shape with the zero background level, which were obtained upon scanning the ECDL frequency over the Doppler profile of the D_2 absorption line of cesium atoms and its coincidence with the ($6S_{1/2}$, $F = 4$) – ($6P_{3/2}$, $F' = 3, 4, 5$) optical transition frequencies, where F and F' are the total angular momenta of the cesium atom in the ground and excited states, respectively. These oscillograms were recorded by changing the only experimental parameter – the modulation frequency, which was equal to 30.1 and 34.3 MHz. The simultaneous change in the shape and the slope of error signals at the fixed modulation frequency is achieved by controlling the phase relation between the input signals of the mixer. This control is performed by simply varying the change of a HF cable connecting the mixer with a generator. The second, the low-frequency feedback loop was used to compensate for slow drifts caused by temperature and mechanical perturbations.

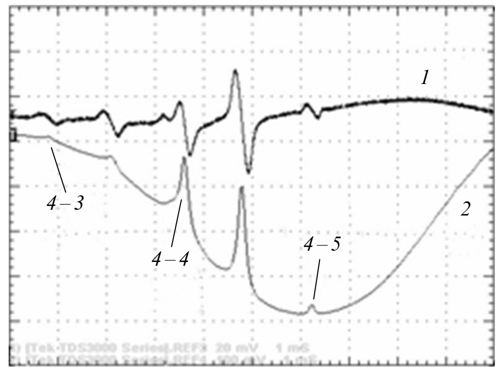

Figure 2. Oscillograms of the error signal (*1*) and saturated absorption signal in the region of the D_2 line of cesium atoms [the ($6P_{3/2}$, $F' = 3, 4, 5$) transition] (*2*) recorded simultaneously with signal (*1*) by PD2. The modulation frequency is 30.1 MHz.

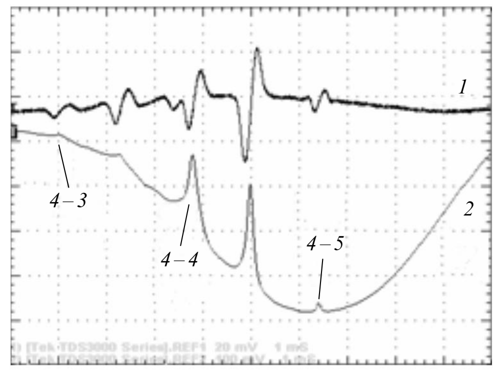

Figure 3. Oscillograms of the error signal (*1*) and saturated absorption signal in the region of the D_2 line of cesium atoms [the ($6S_{1/2}$, $F = 4$) – ($6P_{3/2}$, $F' = 3, 4, 5$) transition] (*2*) recorded simultaneously with signal (*1*) by PD2. The modulation frequency is 34.3 MHz.

The amplified and integrated output signal of the mixer was fed to a piezoceramic transducer controlling the rotation of a diffraction grating.

Note that the FM sideband method, in which an AOM is used as an external phase modulator, gives the same response to noise sources reducing its sensitivity, as in paper [2]. One of the undesirable effects is the presence of the residual amplitude noise caused by the fact that the existing phase modulators do not generate the FM spectrum in a pure form. A weak unbalance between the sideband amplitudes or the relative phase shift of the sidebands can prevent the exact vanishing of the beat signal on a photodetector. Such residual modulation amplitude can be detected with a photodetector to give the nonzero background, whose level can fluctuate together with fluctuations of the laser radiation power. If an EOM is used as an external phase modulator, this noise can be minimised by providing the exact coincidence of polarisations of the input and output radiations to balance the powers of sidebands and also by controlling the relative phase of input signals of the mixer to minimise the background shift caused by the residual amplitude noise. In our case, we did not take care of the radiation polarisation at the AOM input and output. The sidebands are balanced and the background is nullified

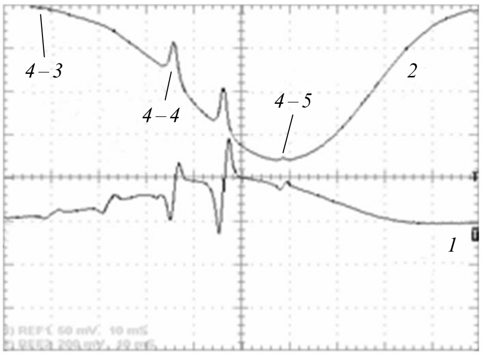

Figure 4. Oscillograms of the error signal (*1*) and saturated absorption signal in the region of the D_2 line of cesium atoms [the ($6S_{1/2}$, $F = 4$) – ($6P_{3/2}$, $F' = 3, 4, 5$) transition] (*2*) recorded simultaneously with signal (*1*) by PD2. The modulation frequency is 23.8 MHz.

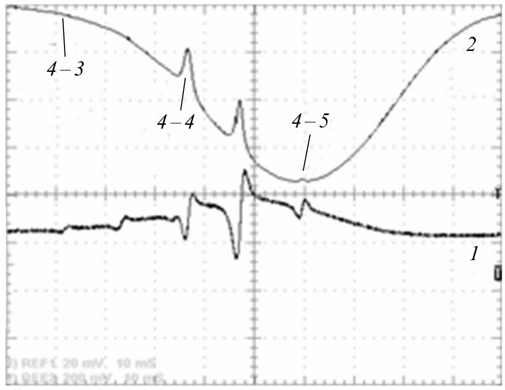

Figure 6. Oscillograms of the error signal (*1*) and saturated absorption signal in the region of the D_2 line of cesium atoms [the ($6S_{1/2}$, $F = 4$) – ($6P_{3/2}$, $F' = 3, 4, 5$) transition] (*2*) recorded simultaneously with signal (*1*)by PD2. The modulation frequency is 12.2 MHz.

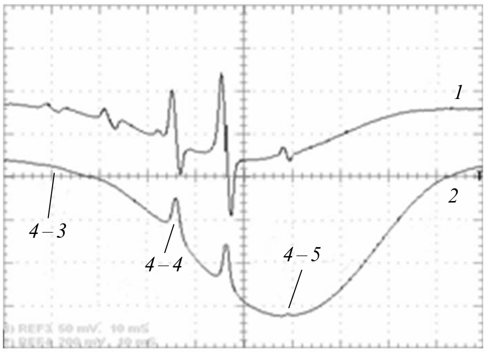

Figure 5. Oscillograms of the error signal (*1*) and saturated absorption signal in the region of the D_2 line of cesium atoms [the ($6S_{1/2}$, $F = 4$) – ($6P_{3/2}$, $F' = 3, 4, 5$) transition] (*2*) recorded simultaneously with signal (*1*) by PD2. The modulation frequency is 26.8 MHz.

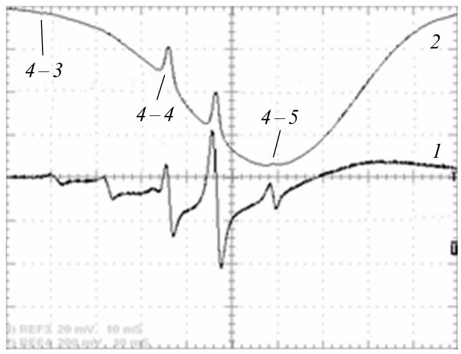

Figure 7. Oscillograms of the error signal (*1*) and saturated absorption signal in the region of the D_2 line of cesium atoms [the ($6S_{1/2}$, $F = 4$) – ($6P_{3/2}$, $F' = 3, 4, 5$) transition] (2) recorded simultaneously with signal (*1*) by PD2. The modulation frequency is 11.2 MHz.

by simply rotating the AOM in the horizontal plane and tuning the HF generator frequency.

After some modification of the experimental setup, mainly due to the replacement of HF cable, we observed the same behaviour of the system (see Figs 2 and 3), but already at the modulation frequencies 23.8 and 26.8 MHz, in the frequency region where the AOM operation efficiency both in the Bragg and Raman – Nath diffraction modes is even lower than that for the modulation frequencies in the case described above (Figs 4 and 5).

Moreover, the high sensitivity of the method is demonstrated by the fact that we obtained error signals for frequencies (about 10 MHz) at which the AOM is not used at all in the Bragg diffraction mode. In this case, the first-order sidebands also vanish almost completely in the Raman – Nath diffraction mode. However, they are still intense enough for using FM spectroscopy at such low modulation frequencies (Figs 6 and 7). Therefore, by changing only modulation frequencies in the region from 10 to 40 MHz without changing the power of a signal fed to the AOM, we can easily distinguish the two FM spectroscopy regimes: when the modulation frequency is so high that only one sideband efficiently interacts with an absorbing medium [2] or when the distance between sidebands is comparable with the width of sub-Doppler resonances [1].

Because the detection units of the electronic system should be shielded from the action of HF electromagnetic radiation scattered, for example, by a high-power amplifier powering the AOM, the use of lower modulation frequencies seems preferable.

To tune the ECDL frequency to the maximum of the saturated absorption line, we used two electronic feedback loops, slow and fast, in the automatic frequency control system. The slow, narrowband loop is used to suppress low-frequency noise caused by external acoustic and mechanical perturbations and to eliminate slow temperature drifts of the ECDL cavity length by controlling the voltage applied to a piezoceramic transducer. The fast loop with a broad (in our case, 6 MHz at the 3-dB level) tuning band produces the correction signal, which is summed with the current of the LD power supply.

Figure 8 shows the simplified principal scheme of the feedback loop in the LD injection current. The output signal of the mixer, which is the error signal of our automatic frequency control system, is passed through a low-frequency filter to eliminate residual signals at the HF generator frequency and its second harmonic and then is fed to the inputs of both feedback loops. The slope of the error signal can be varied by changing simply the HF generator frequency. In addition, we can change the slope of the

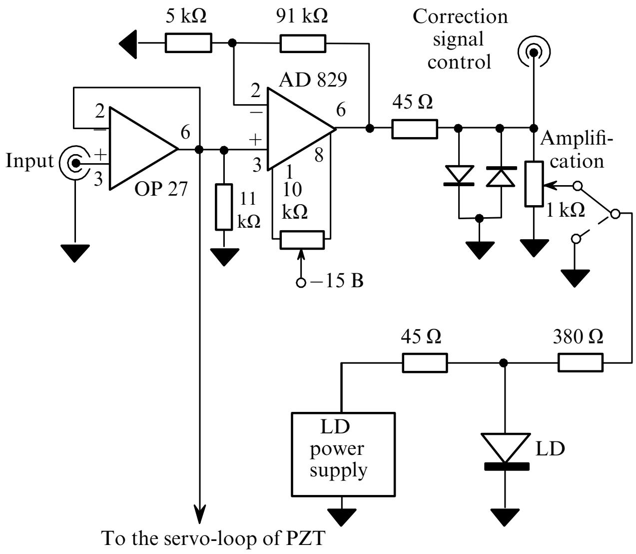

Figure 8. Electric circuit of the LD injection-current feedback loop.

loop-correction signal controlling the rotation angle of a diffraction grating. As a result, a correct relation is achieved between the slopes of correction signals for the injection current and voltage of the power supply of the piezoceramic transducer.

To determine the optimal amplification of the output correction signal for the fast servo-loop for frequency locking by the injection current, we performed the fast Fourier transform (FTT) [FTT is the measuring regime of a Tektronix 3014B oscilloscope] of the correction signals for the slow and fast servo-loops. When the laser frequency was tuned to the peak of an optical resonance and the LD injection current feedback loop was opened, we amplified the slow-loop correction signal until the piezoceramic transducer began oscillate at the frequency close to 1.5 kHz, and noise frequency components caused by excitation of the loop appeared in the spectra of both correction signals [curves (*1*) in Figs 9 and 10]. By closing the fast loop and increasing gradually (from zero) the correction signal of the LD injection current, we observed the broadband suppression of this noise [curves (*2*) in Figs 9 and 10].

Thus, the error signal is an excellent indicator of the level and spectral characteristics of compensated noises and the tuning bandwidth feedback loops. For example, at the modulation frequency 39.6 MHz, the spectrum of the

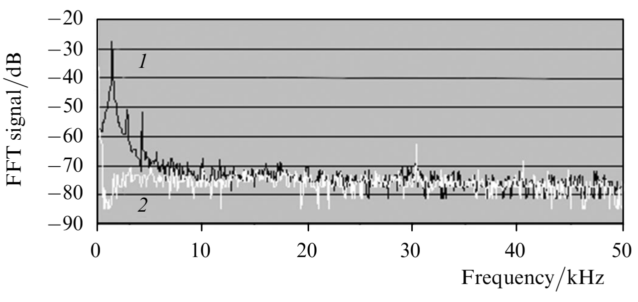

Figure 9. Spectrum of the feedback-loop correction signal by the voltage across a piezoelectric transducer for the open (*1*) and closed (*2*) LD injection-current feedback loop. The AOM modulation frequency is 40 MHz.

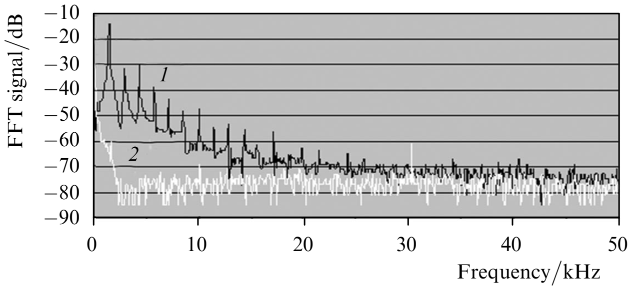

Figure 10. Spectrum of the feedback-loop correction signal by the LD injection current for the open (*1*) and closed (*2*) feedback loop. The AOM modulation frequency is 40 MHz.

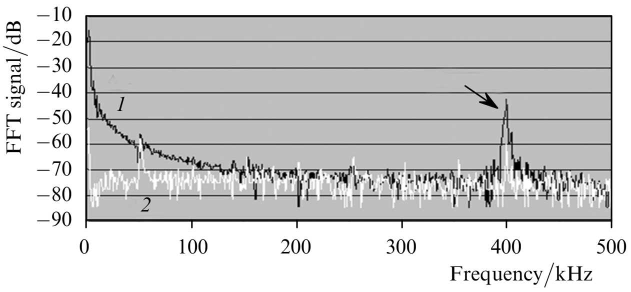

Figure 11. Spectrum of the feedback-loop correction signal by the LD injection current for the open (*1*) and closed (*2*) feedback loop. The AOM modulation frequency is 39.6 MHz.

correction signal for the fast loop [curve (*1*) in Fig. 11] exhibits, along with noise caused by oscillations in the slow loop, the noise component at the frequency $\sim$400 kHz (indicated by the arrow in Fig. 11), which was suppressed after closing the fast loop [curve (*2*)].

Having at present only one laser system described in the paper, we cannot estimate reliably the width of the ECDL emission spectrum. The analysis of the spectrum of beats between radiation frequencies of our laser system and a Topica DL 100 commercial system (Germany) by repeating the above-described procedure, i.e. upon intentional excitation of the slow servo-loop (resulting in the appearance of the frequency components in the beat spectrum in the band up to 10 MHz with respect to the frequency of the central beat signal of width $\sim$2 MHz at the 3-dB level) followed by closing the fast loop and suppression of the induced components, showed that the width of the tuning band of our laser system can be a few megahertz. The DL 100 laser system is a diode laser with the external cavity formed by a diffraction grating and the injection current modulated at frequencies up to 14 kHz.

In our opinion, the spatial divergence of the output radiation of the AOM, i.e. of the beams corresponding to the carrier and nearest sidebands of the $\pm$1st diffraction orders does not prevent considerably the use of the resonances of a high-Q Fabry–Perot interferometer (instead of atomic resonances) as frequency discriminators in the FM Pound–Drever spectroscopy. Figure 12 shows the scheme of the experimental setup which we used to obtain input signals for a mixer in this case. For the appropriate focal distances of lenses L1 and L2 forming a telescopic system with an AOM located between them, the input radiation of the cavity represents three collimated and parallel beams corresponding to the carrier and sidebands of the $\pm$1st

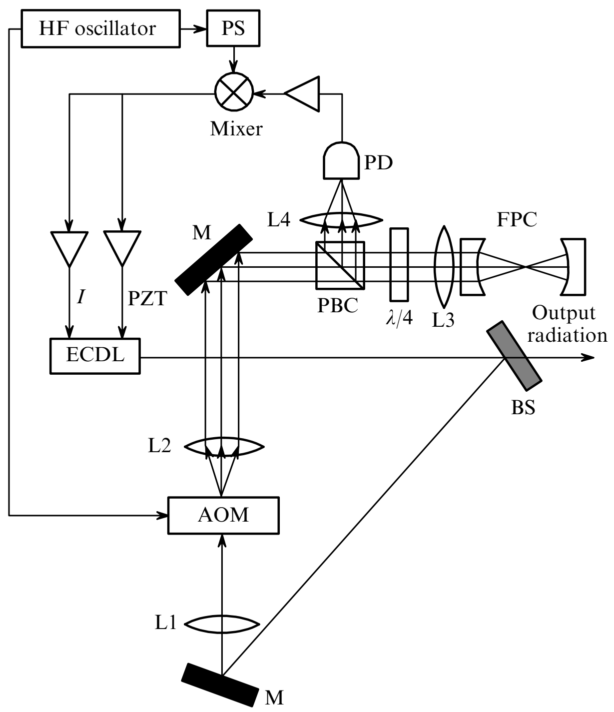

Figure 12. Scheme of the experimental setup with a Fabry–Perot resonator as a frequency discriminator: (PZT) piezoceramic transducer; (PS) phase shifter; (BS) beamsplitter; (PBC) polarisation beamsplitter cube; (L1–L4) lenses; (PD) photodetector; (FPC) Fabry–Perot cavity; ($\lambda/4$) quarter-wave plate; (M) mirror; (I) injection current.

diffraction orders. B varying, as before, the modulation frequency of the AOM, we observed again a change in the slope of error signals at different frequencies in the region from 10 to 40 MHz.

3. Conclusions

We have performed phase-sensitive detection of atomic resonances by the FM Pound–Drever technique in which an AOM operating in the Raman–Nath diffraction mode is used. A simple and efficient method of frequency control by FM sidebands by using the AOM as an external phase modulator can be employed to obtain error signals (in a broad frequency range of the AOM) in extremely high-speed injection-current negative-feedback loops by frequency locking of an ECDL to atomic resonances or high-Q optical cavity resonances. The method eliminates the problems related to frequency noises introduced upon direct frequency modulation of the LD injection current and broadens the tuning band of the injection-current feedback loop (in the megahertz range), thereby narrowing the emission spectrum of the laser.

References

1. Drever R., Hall J., Kovalski F., Hough J., Ford G., Munley A., Ward H. *Appl. Phys. B*, **31**, 97 (1983).
2. Bjorklund G., Levenson M., Lenth W., Ortiz C. *Appl. Phys. B*, **32**, 145 (1983).
3. Barychev V. *Proc. 4-th Int. Symp. on Modern Problems of Laser Physics (MPLP 2004)* (Novosibirsk, Russia, 2004) p. 260.
4. Dieulesaint E., Royer D. *Elastic Waves in Solids* (New York: Wiley, 1981; Moscow: Nauka, 1982).